

# Minority Oversampling for Imbalanced Time Series Classification

Tuanfei Zhu<sup>1</sup>, Cheng Luo<sup>3</sup>, Jing Li<sup>1</sup>, Siqi Ren<sup>4</sup> and Zhihong Zhang<sup>2,\*</sup>

<sup>1</sup>College of Computer Engineering and Applied Mathematics, Changsha University, Changsha, 410000, China

<sup>2</sup>School of Information Technology and Management, Hunan University of Finance and Economics, Changsha, 410205, China

<sup>3</sup>School of Information Engineering, Jiangxi Vocational Technical College of Industry and Trade, Nanchang, 330038, China

<sup>4</sup>School of Computer and Information Engineering, Zhejiang Gongshang University, Hangzhou, 310000, China

\*Corresponding Author: Zhihong Zhang. Email: zhzhong@ccsu.edu.cn

Received: XX Month 202X; Accepted: XX Month 202X

**Abstract:** Many important real-world applications involve time-series data with skewed distribution. Compared to conventional imbalance learning problems, the classification of imbalanced time-series data is more challenging due to high dimensionality and high inter-variable correlation. This paper proposes a structure preserving Oversampling method to combat the High-dimensional Imbalanced Time-series classification (OHIT). OHIT first leverages a density-ratio based shared nearest neighbor clustering algorithm to capture the modes of minority class in high-dimensional space. It then for each mode applies the shrinkage technique of large-dimensional covariance matrix to obtain accurate and reliable covariance structure. Finally, OHIT generates the structure-preserving synthetic samples based on multivariate Gaussian distribution by using the estimated covariance matrices. Experimental results on several publicly available time-series datasets (including unimodal and multimodal) demonstrate the superiority of OHIT against the state-of-the-art oversampling algorithms in terms of F1, G-mean, and AUC.

**Keywords:** Imbalanced learning; oversampling; classification; clustering

## 1 Introduction

The imbalanced learning problem appears when the distribution of samples is significantly unequal among different classes. The majority class with relatively more samples can overwhelm the minority class in sample size. Since standard machine learning methods usually seek the minimization of training errors, the resulting classifiers will be naturally biased towards the majority class, leading to the performance depreciation for important and interest minority samples [1-2]. Over the past two decades, a large number of class imbalance techniques have been proposed to combat the imbalanced data learning [2-6]. These existing solutions can be roughly divided into algorithm-level approaches and data-level approaches.

In algorithm-level approaches, traditional classification algorithms are improved to put more emphasis on the learning of minority class by adjusting training mechanism or prediction rule such as modification of loss function [5], introduction of class-dependent costs [1], and movement of output threshold [6]. Data-level approaches aim to establish class balance by adding new minority samples (i.e., oversampling) [2, 7-10], deleting a part of original majority samples (i.e., undersampling) [3], or combining both of them. Compared to algorithm-level methods, data-level techniques have two main advantages. First, they are more universal, since the preprocessed data can be fed into various machine learning algorithms to boost their prediction capability in the minority class. Second, data-level

approaches can flexibly integrate with other techniques such as kernel methods and ensemble learning to explore elaborate hybrid solutions [3, 9].

In this paper, we focus our attention on oversampling techniques in data-level approaches, since oversampling directly addresses the difficulty source of classifying imbalanced data by compensating the insufficiency of minority class information, and, unlike undersampling, does not suffer the risk of discarding informative majority samples.

### ***1.1 Motivation***

The problem of imbalanced time series classification is frequently encountered in many real-world applications, including medical monitoring, abnormal movement detection, and industrial hazards surveillance. Although there are a large number of oversampling solutions in previous literature, few of them are exclusively designed to deal with imbalanced time-series data. Different from conventional data, time series data presents high dimensionality and high inter-variable correlation, as time-series sample is an ordered variable set which is extracted from a continuous signal. As a result, addressing imbalanced time series classification exist some special difficulties as compared to classical class imbalance problems [10-11]. In terms of data oversampling, the designed oversampling algorithm should have the capability of coping with the additional challenges due to high dimensionality, and protect the original correlation among variables so as not to confound the learning.

Therefore, we want to develop an oversampling method for imbalanced time series data that can accurately acquire the correlation structure of minority class, and generate structure-preserving synthetic samples to maintain the main correlation implied in the minority class. The purpose is to greatly improve the performance of minority class without seriously damaging the classification accuracy on the majority class.

### ***1.2 Limitations of Existing Techniques***

In the past two decades, a large number of oversampling methods were proposed to handle imbalanced learning problems, where interpolated techniques, probability distribution-based methods, and structure preserving approaches are three main types of oversampling.

In interpolation oversampling, the synthetic samples are randomly interpolated between the feature vectors of two neighboring minority samples [2, 7-8]. Because of the high dimensionality of time-series data, there may exist a considerable space between arbitrary two time-series minority samples. When the synthetic samples are allowed to create in such of the region, they seem to scatter in the whole feature space, which leads to severe over-generalization problem. In addition, interpolated oversampling methods can introduce a lot of random data variations since they only take the local characteristics of minority samples into account. It will weaken the inherent correlation of original time-series data.

For probability distribution-based methods, they first estimate the underlying distribution of minority class, then yield the synthetic samples according to the estimated distribution [12-14]. However, accurate discrete probability distribution or probability density function is extremely hard to obtain due to the scarcity of minority samples, especially in high-dimensional space [15].

Structure-preserving oversampling methods generate the synthetic samples on the premise of reflecting the main structure of minority class. In paper [16], the authors proposed Mahalanobis Distance-based Oversampling (MDO). MDO produces the synthetic samples which obey the sample covariance structure of minority class by operating the value range of each feature in principal component space. The major drawback of MDO is that the sample covariance matrix can seriously deviate from the true covariance one for high-dimensional data, i.e., the smallest (/largest) eigenvalues of sample covariance matrix can be greatly underestimated (/overestimated) compared to the corresponding true eigenvalues [17]. Different from MDO, the structure-preserving oversampling methods SPO [10] and INOS [11] first divide the eigenspectrum of sample covariance matrix into the reliable and unreliable subspaces, then pull up the sample eigenvalues in unreliable subspace. However, both SPO and INOS assume the minority

class is unimodal. This assumption often does not hold for real-life data, since the samples of a single class may imply multiple modes (e.g., the failure events of aircrafts exist multiple failure modes; a disease includes distinct subtypes). To handle the multimodal minority class, Pang et al. developed a parsimonious Mixture of Gaussian Trees models (MoGT) which attempts to construct Gaussian graphical model for each mode [18]. However, MoGT only considers the correlations among pairs of nearest variables in order to reduce the number of estimated parameters. Besides, MoGT does not build the reliable mechanism to identify the modes of minority class. The authors, in fact, set the number of mixture components manually.

### ***1.3 Our Method and Main Contributions***

Based on the above analyses, existing oversampling algorithms cannot protect the structure of minority class well for imbalanced time series data, especially when the minority class is multimodal. In this study, we propose a structure-preserving oversampling method OHIT which can accurately maintain the covariance structure of minority class and deal with the multimodality simultaneously. OHIT leverages a Density-Ratio based Shared Nearest Neighbor clustering algorithm (DRSNN) to cluster the minority class samples in high-dimensional space. Each discovered cluster corresponds to the representative data of a mode. To overcome the problem of small sample and high dimensionality, OHIT for each mode use the shrinkage technique to estimate covariance matrix. Finally, the structure-preserving synthetic samples are generated based on multivariate Gaussian distribution by using the estimated covariance matrices.

The major contributions of this paper are as follows: 1) We design a robust DRSNN clustering algorithm to capture the potential modes of minority class in high-dimensional space. 2) We improve the estimate of covariance matrix in the context of small sample size and high dimensionality, through utilizing the shrinkage technique based on Sharpe’s single-index model. 3) The proposed OHIT is evaluated on both the unimodal datasets and multimodal datasets; the results show that OHIT has better performance than existing representative methods.

The remainder of this paper is organized into five sections. The proposed OHIT framework is presented in Section 2. In Section 3, the experimental study and results are given. Finally, we conclude the paper and some future research directions in Section 4.

## **2 The Proposed OHIT Framework**

OHIT involves three key issues: 1) clustering high-dimensional data; 2) estimating the large-dimensional covariance matrix based on limited data; 3) and yielding structure-preserving synthetic samples. In section 3.1, we introduce the clustering of high-dimensional data, where a new clustering algorithm DRSNN is presented. Section 3.2 describes the shrinkage estimation of covariance matrix. The shrinkage covariance matrix is a more accurate and reliable estimator than the sample covariance matrix in the context of limited data. Section 3.3 gives the generation of structure-preserving synthetic samples.

### ***2.1 Clustering of High-dimensional Data***

#### ***2.1.1 Preliminary***

Two significant challenges exist in clustering high-dimensional data. First, the distances or similarities between samples tend to be more uniform, which can weaken the utility of similarity measures for discrimination, causing clustering more difficult. Second, clusters usually present different densities, sizes, and shapes.

Some research works developed Shared Nearest Neighbor similarity (SNN)-based density clustering methods to cluster high-dimensional data [32-33]. In density clustering, the concept of core point can help to solve the problems of clusters with different sizes, shapes. In SNN similarity, the similarity between a pair of samples is measured by the number of the common neighbors in their nearest neighbor lists [34].

Since the rankings of the distances are still meaningful in high-dimensional space, SNN is regarded as a good secondary similarity measure for handling high-dimensional data [35]. Furthermore, given that SNN similarity only depends on the local configuration of the samples in the data space, the samples within dense clusters and sparse clusters will show roughly equal SNN similarities, which can mitigate the difficulty of clustering caused by the density variations of clusters.

The main phases of SNN clustering approaches can be summarized as follows: 1) defining the density of sample based on SNN similarity; 2) finding the core points according to the densities of samples, and then defining directly density-reachable sample set for them; 3) building the clusters around the core points. Below, we describe the key concepts associated with these phases, respectively.

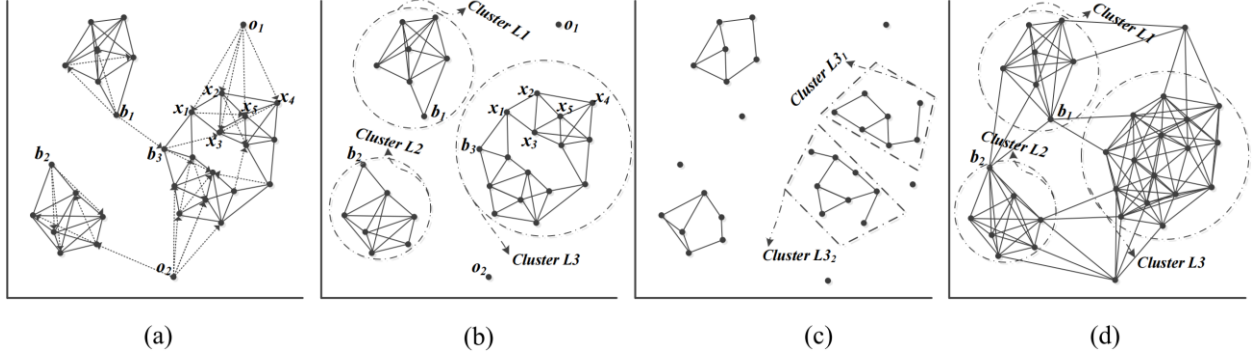


**Figure 1:** (a) Figures illustrating a nearest neighbor graph with  $k = 5$ . (b), (c) and (d) Figures illustrating the shared nearest neighbor graph when  $k$  is 5, 3 and 10, respectively.

**SNN similarity and the density of sample.** For two samples  $x_i$  and  $x_j$ , their SNN similarity is given as follows,

$$SNN(x_i, x_j) = |N_k(x_i) \cap N_k(x_j)| \quad (1)$$

where  $N_k(x_i)$  and  $N_k(x_j)$  are respectively the  $k$ -nearest neighbors of  $x_i$  and  $x_j$ , determined by certain primary similarity or distance measure (e.g.,  $L_p$  norm).

In traditional density clustering, the density of a sample is defined as the number of the samples whose distances from this sample are not larger than the distance threshold  $Esp$  [36]. If this definition is extended to SNN clustering, the density of a sample  $x_i$ ,  $de(x_i)$ , can be expressed as [32]:

$$de(x_i) = \sum_{x \in SN_k(x_i)} SNN(x_i, x) * 1\{SNN(x_i, x) \geq Esp\} \quad (2)$$

where  $SN_k(x_i)$  is  $x_i$ 's  $k$ -nearest neighbors according to SNN similarity,  $1\{\cdot\}$  is an indicator function (it returns 1 if the relational expression is true, otherwise, 0 is returned). However, this kind of definition can make outliers and normal samples being nondiscriminatory in density [33].

Consider Fig. 1a, the outliers  $o_1$  and  $o_2$  all have a considerable overlap degree of neighborhoods with their nearest neighbors. Hence,  $o_1$  and  $o_2$  are also high density according to Eqn. 2. To solve this problem, Eqn. 2 can be modified as

$$de(x_i) = \sum_{x \in SN_k(x_i)} SNN(x_i, x) * J(x, x_i, Esp) \quad (3)$$

where  $J(x, x_i, Esp)$  is  $1\{x_i \in SN_k(x)\} * 1\{SNN(x_i, x) \geq Esp\}$ . Eqn.3 indicates only the samples occurred in the  $k$  nearest neighbor lists each other can contribute the similarity into their densities. Fig. 1b shows the corresponding shared nearest neighbor graph of Fig. 1a. From this figure, we can see that the outliers ( $o_1$  and  $o_2$ ) and their neighboring samples does not form pairs of shared nearest neighbors (i.e., there are no links), the densities of  $o_1$  and  $o_2$  tend to be 0; at the same time, the links of the border samples such as  $b_1, b_2$  and  $b_3$  are relatively sparse, their densities will be naturally lower than the densities of the samples within clusters. Eqn. 3 can benefit to obtain a more reasonable distribution of sample density.

**Core points and directly density-reachable sample set.** In SNN clustering, the core points are the samples whose densities are higher the density threshold  $MinPts$ , and the directly density-reachable

sample set of a core point is defined as those shared nearest neighbors which the similarities with this core point exceed  $Esp$  [33].

**The creation of clusters.** The core points, that are directly density-reachable each other, are put into the same clusters; all the samples that are not directly density-reachable with any core points are categorized as outliers (or noisy samples); and the non-core and non-noise points are assigned to the clusters in which their nearest core points are.

### 2.1.2 DRSNN: A Density Ratio-based Shared Nearest Neighbor Clustering Method

$MinPts$  and  $Esp$  are two important parameters in SNN clustering, but, as we know, there is no general principle to set the “right” values for them [33]. In addition, SNN clustering is also sensitive to the neighbor parameter  $k$  [33-34]. If  $k$  is set to be small, a complete cluster may be broken up into several small pieces, due to the limited density-reachable samples and the local variations in similarity. Consider Fig. 1c where the parameter  $k$  is set 3. The directly density-reachable sets of the points in the blocks  $L3_1$  and  $L3_2$  are restricted in the respective blocks,  $L3_1$  and  $L3_2$  cannot be combined into the integrated cluster  $L3$ . On the other hand, if  $k$  is too large such as being greater than the size of clusters, multiple clusters are prone to merge into a cluster, as the changes of density in transition regions will not have a substantially effect for separating different clusters. As shown in Fig. 1d where the shared nearest neighbors graph is presented when  $k$  is 10. The border points  $b_1$  and  $b_2$  contain the points from different clusters in their directly density-reachable sets, and show roughly equal densities with the points inside of the clusters (i.e., easy to be the core points). Hence,  $L1$ ,  $L2$ , and  $L3$  tend to form a uniform cluster. In conclusion, the major drawback of SNN clustering is hard to set the appropriate values for the parameters, causing unsteady performance of clustering.

To solve the problem mentioned above, we propose a new clustering method based on Density Ratio and SNN similarity, DRSNN. We first present the key components in DRSNN, and then summarize the algorithm process of DRSNN.

**The density of sample.** To avoid the use of  $Esp$ , DRSNN defines the density of a sample as the sum of the similarity between this sample and each of its shared nearest neighbors. Formally, the density of the considered sample  $x_i$ ,  $de(x_i)$ , is

$$de(x_i) = \sum_{x \in SN_k(x_i)} (SNN(x_i, x) * 1\{x_i \in SN_k(x)\}) \quad (4)$$

**The density ratio of sample and the identification of core point.** Instead of finding the core points based on the density estimate, DRSNN uses the estimate of density ratio [37]. Specifically, the density ratio of a sample is the ratio of the density of this sample to the average density value of  $\kappa$ -nearest neighbors of this sample,

$$dr(x_i) = de(x_i) / \frac{1}{\kappa} \sum_{x \in SN_\kappa(x_i)} de(x) \quad (5)$$

The core points can be defined as the samples whose density ratios are not lower a threshold value  $drT$ . The use of density ratio has the following advantages. 1) It facilitates to identify core points. Given that the core points are the samples with local high densities, the density-ratio threshold  $drT$  can be set to around 1. 2) The parameter  $MinPts$  can be eliminated. 3) The density ratios of samples are not affected by the variations of clusters in density.

**Directly density-reachable sample set.** In DRSNN, we define the directly density-reachable sample set for the core point as follows:

$$H_k(x_i) = \{x_i\} \cup SN_\kappa(x_i) \cup \{x_j \in RSN_\kappa(x_i) | x_j \text{ is a core sample}\} \quad (6)$$

where  $RSN_\kappa(x_i)$  is  $x_i$ 's reverse  $\kappa$ -nearest neighbors set. The directly density-reachable set  $H_k(x_i)$  mainly includes two parts, i.e., the  $\kappa$ -nearest neighbors of  $x_i$  and the core points in the reverse  $\kappa$ -nearest neighbors of  $x_i$ . The definition of  $H_k(\cdot)$  is based on two considerations. One is that the samples distributed closely around a core point should be directly density-reachable with this core point. The other one is to assure that  $H_k(\cdot)$  satisfies reflexivity and symmetry, which is a key condition that DRSNN can deterministically

discover the clusters of arbitrary shape [38]. Note that the parameter  $\kappa$  can restrain the merger of clusters by using a small value to shrink directly density-reachable sample set, and reduce the risk of splitting the clusters by employing a large value to augment the set of directly density-reachable samples.

**The summary of DRSNN algorithm.** DRSNN algorithm can be summarized as follows:

- 1) Find  $k$ -nearest neighbors of minority samples according to certain primary distance measure.
- 2) Calculate SNN similarity for all pairs of minority samples based on Eqn. 1.
- 3) Calculate the density of each minority sample as Eqn. 4.
- 4) Calculate the density ratio of each minority sample as Eqn. 5.
- 5) Identify the core points, i.e., all the minority samples that have a density ratio greater than  $drT$ .
- 6) Find the directly density-reachable sample set for each core point as Eqn. 6.
- 7) Build the clusters. The core points, that are directly density-reachable each other, are placed in the same clusters; the samples which are not directly density-reachable with any core points are treated as outliers; finally, all the other points are assigned to the clusters where their directly density-reachable core points are.

Although DRSNN also contains three parameters (i.e.,  $drT$ ,  $k$  and  $\kappa$ ), it is capable of selecting the proper value for  $drT$  around 1. In addition,  $k$  and  $\kappa$  can be set in complementary way to avoid the mergence and dissociation of clusters, i.e., a large  $k$ , compared to the number of samples, with a relative low  $\kappa$ , while a small  $k$  accompanied by a relative high  $\kappa$ .

## 2.2 Shrinkage Estimation of Large-dimensional Covariance Matrix

In the setting of high dimensionality and small sample, the sample covariance matrix is not anymore an accurate and reliable estimate of the true covariance matrix  $\Sigma$  [17]. The shrinkage technique, as one of the most common methods improving the estimate of covariance matrix, aims to linearly combine the unrestricted sample covariance matrix  $\mathbf{S}$  and a constrained target matrix  $\mathbf{F}$  to yield a shrinkage estimator with less estimation error [39-40], i.e.,

$$\mathbf{S}^* = \alpha\mathbf{F} + (1 - \alpha)\mathbf{S} \quad (7)$$

where  $\alpha \in [0, 1]$  is the weight assigned to the target matrix  $\mathbf{F}$ , called the shrinkage intensity. Since there are a lot of estimated parameters in  $\mathbf{S}$  and a limited amount of data, the unbiased  $\mathbf{S}$  will exhibit a high variance, whereas the preset  $\mathbf{F}$  will have relatively low variance but potentially high bias as it is presumed to impose certain low-dimensional structure. The shrinkage technique can acquire more precise estimate for  $\Sigma$  by taking a properly trade-off between  $\mathbf{S}$  and  $\mathbf{F}$  [40].

A key question is how to find the optimal shrinkage intensity. Once  $\alpha$  is obtained, the shrinkage estimator  $\mathbf{S}^*$  can be determined. A popular solution is to analytically choose the value of  $\alpha$  by minimizing Mean Squared Error (MSE) [41]. The advantages of this way are that the resulting estimator is distribution-free and inexpensive in computational complexity. Specifically, the MSE can be expressed as the squared Frobenius norm of the difference between  $\Sigma$  and  $\mathbf{S}^*$ ,

$$L(\alpha) = \|\alpha\mathbf{F} + (1 - \alpha)\mathbf{S} - \Sigma\|^2 \quad (8)$$

which leads to the risk function

$$\begin{aligned} R(\alpha) &= E(L(\alpha)) = \sum_{i=1}^d \sum_{j=1}^d E(\alpha f_{ij} + (1 - \alpha)s_{ij} - \sigma_{ij})^2 \\ &= \sum_{i=1}^d \sum_{j=1}^d \text{Var}(\alpha f_{ij} + (1 - \alpha)s_{ij}) + [E(\alpha f_{ij} + (1 - \alpha)s_{ij} - \sigma_{ij})]^2 \\ &= \sum_{i=1}^d \sum_{j=1}^d \alpha^2 \text{Var}(f_{ij}) + (1 - \alpha)^2 \text{Var}(s_{ij}) + 2\alpha(1 - \alpha) \text{Cov}(f_{ij}, s_{ij}) + [\alpha E(f_{ij}, s_{ij}) + \text{Bias}(s_{ij})]^2 \quad (9) \end{aligned}$$

$f_{ij}$ ,  $s_{ij}$  and  $\sigma_{ij}$  are the elements of  $\mathbf{F}$ ,  $\mathbf{S}$  and  $\Sigma$ , respectively;  $d$  is the dimension of feature. Since  $\mathbf{S}$  is an unbiased estimator of  $\Sigma$ ,  $\text{Bias}(s_{ij})$  is actually 0.

Computing the first and two derivatives of  $R(\alpha)$  yields the following equations:

$$R'(\alpha) = 2 \sum_{i=1}^d \sum_{j=1}^d \alpha \text{Var}(f_{ij}) - (1 - \alpha) \text{Var}(s_{ij}) + (1 - 2\alpha) \text{Cov}(f_{ij}, s_{ij}) + \alpha (E(f_{ij} - s_{ij}))^2 \quad (10)$$

$$R''(\alpha) = 2 \sum_{i=1}^d \sum_{j=1}^d \text{Var}(f_{ij} - s_{ij}) + (E(f_{ij} - s_{ij}))^2 \quad (11)$$

By setting  $R'(\alpha) = 0$ , we can obtain

$$\alpha^* = \frac{\sum_{i=1}^d \sum_{j=1}^d \text{Var}(s_{ij}) - \text{Cov}(f_{ij}, s_{ij})}{\sum_{i=1}^d \sum_{j=1}^d E[(f_{ij} - s_{ij})^2]} \quad (12)$$

$R''(\alpha)$  is positive according to Eqn. 11. Hence,  $\alpha^*$  is a minimum solution of  $R(\alpha)$ . Following [40], we replace the items of expectations, variances, and covariances in Eqn. 12 with their unbiased sample counterparts, which gives rise to

$$\hat{\alpha}^* = \frac{\sum_{i=1}^d \sum_{j=1}^d \widehat{\text{Var}}(s_{ij}) - \widehat{\text{Cov}}(f_{ij}, s_{ij})}{\sum_{i=1}^d \sum_{j=1}^d (f_{ij} - s_{ij})^2} \quad (13)$$

For the preset  $\mathbf{F}$ , the covariance matrix implied in Sharpe's single-index model is used [42]. The single-index model is used to forecast stock returns from time-series stock exchange data. In this case,  $\mathbf{F}$  can be expressed by  $\mathbf{S}$  as follows,

$$f_{ij} = \begin{cases} s_{ij} & \text{if } i = j \\ \sqrt{s_{ii}s_{jj}} & \text{otherwies.} \end{cases} \quad (14)$$

Putting Eqn. 14 into Eqn. 13, an expression of  $\hat{\alpha}^*$ , that only contains the elements of sample covariance matrix, can be obtain finally

$$\hat{\alpha}^* = \frac{\sum_{i \neq j} \widehat{\text{Var}}(s_{ij}) - t_{ij}}{\sum_{i \neq j} (\sqrt{s_{ii}s_{jj}} - s_{ij})^2} \quad (15)$$

where  $t_{ij} = \frac{1}{2} [\sqrt{s_{jj}/s_{ii}} \widehat{\text{Cov}}(s_{ii}, s_{ij}) + \sqrt{s_{ii}/s_{jj}} \widehat{\text{Cov}}(s_{jj}, s_{ij})]$ .

Given that the value of  $\hat{\alpha}^*$  may be greater (/smaller) than 1 (/0) due to limited samples,  $\hat{\alpha}^{**} = \max(0, \min(1, \hat{\alpha}^*))$  is adopted in practice.

### 2.3 Generation of Structure-preserving Synthetic Samples

The generation of synthetic samples of OHIT is simple. For a cluster  $i$  discovered by DRSNN, we first compute its mean of cluster ( $\mu_i$ ) and shrinkage covariance matrix ( $\mathbf{S}_i^*$ ), then the synthetic samples are yielded based on the Gaussian distribution  $N(\mu_i, \mathbf{S}_i^*)$ . In this way, the synthetic samples can maintain the covariance structure of each mode.

---

#### Algorithm 1 OHIT( $P, k, \kappa, drT, \eta$ )

---

**Require:**  $P$ : the minority sample set;  $k, \kappa, drT$ : three parameters in DRSNN clustering;  $\eta$ : the number of synthetic samples required to be generated;

**Ensure:**  $Syn$ : the generated synthetic sample set

- 1: Employ DRSNN to cluster the minority class sample set,  $C_i \leftarrow \text{DRSNN}(P, k, \kappa, drT)$ ,  $i = 1, 2, \dots, m$ , where  $m$  is the number of discovered clusters.
  - 2: Compute the shrinkage covariance matrix  $\mathbf{S}_i^*$  for each cluster  $C_i$  by combining Eqns. 7, 14, and 15.
  - 3: Generate the synthetic sample set  $Syn_i$  with size  $\left\lceil \eta \frac{|C_i|}{|P|} \right\rceil$  for each cluster  $C_i$  based on  $N(\mu_i, \mathbf{S}_i^*)$ , then add  $Syn_i$  into  $Syn$ .
- 

## 3 Experimental Results and Discussion

### 3.1 Experimental Setting

**Experimental Datasets.** We construct two groups of binary imbalanced datasets from UCR time series repository [43]. For the first group, the minority class of each dataset is the smallest original class in the data, and the majority class consists of all the remaining original classes. We call this group the “unimodal” data group, where “unimodal” refers to that the minority class is formed by only one original class [18]. Table 1 presents the data characteristics of this group. It is worth pointing out that all the binary datasets whose imbalance ratios are higher than 1.5 in 2015 UCR repository have been added into this group, including Hr, Sb, POC, Lt2, PPOC, E200, Eq, and Wf.

For the second group, the minority class of each dataset is constructed by merging two or three smallest original classes, and the majority class is composed of the remaining original classes. If the small original classes have very limited samples, we combine three smallest original classes into the minority class. Otherwise, two smallest original classes are merged. The datasets of this group are to simulate the scenario that the minority class is indeed multimodal. We call them the multimodal data group. Since our OHIT considers the multimodality of minority class, OHIT is expected to perform well on this group. Table 2 summarizes the data characteristics of this group, where the feature dimension is greater than the number of minority samples on all the datasets.

**Assessment metrics.** In imbalanced learning area, F1 and G-mean are two widely used comprehensive metrics which can reflect the compromised performance on the majority class and minority class. The definitions of them are as follows:

$$F1 = \frac{2 \cdot \text{Recall} \cdot \text{Precision}}{\text{Recall} + \text{Precision}} \quad G - \text{mean} = \sqrt{\text{Recall} \cdot \text{Specificity}} \quad (16)$$

where Recall and Precision are the measures of completeness and exactness on the minority class, respectively; Specificity is the measure of prediction accuracy on the majority class. Another popular overall metric is the Area Under the receiver operating characteristics Curve (AUC) [44]. Unlike F1 and G-mean, AUC is not affected by the decision threshold of classifiers. In this paper, we use F1, G-mean, and AUC to assess the performance of algorithms.

**Table 1:** Summary of the imbalanced unimodal time-series datasets used in the experiments

Dataset	Minority Class	Length	Training data		Testing data	
			Class Distribution	IR	Class Distribution	IR
Yoga (Yg)	'1'	426	137/163	1.19	1393/1607	1.15
Herring (Hr)	'2'	512	25/39	1.56	26/38	1.46
Strawberry (Sb)	'1'	235	132/238	1.8	219/394	1.8
PhalangesOutlinesCorrect (POC)	'0'	80	628/1172	1.87	332/526	1.58
Lighting2 (Lt2)	'-1'	637	20/40	2	28/33	1.18
ProximalPhalanxOutlineCorrect (PPOC)	'0'	80	194/406	2.09	92/199	2.16
ECG200 (E200)	'-1'	96	31/69	2.23	36/64	1.78
Earthquakes (Eq)	'0'	512	35/104	2.97	58/264	4.55
Two_Patterns (Tp)	'2'	128	237/763	3.22	1011/2989	2.96
Car	'3'	577	11/49	4.45	19/41	2.16
ProximalPhalanxOutlineAgeGroup (PPOA)	'1'	80	72/328	4.56	17/188	11.06
Wafer (Wf)	'-1'	152	97/903	9.3	665/5499	8.27

IR is the imbalance ratio (#majority class samples/#minority class samples).

**Table 2:** Summary of the imbalanced multimodal time-series datasets used in the experiments

Dataset	Minority class	Length	Training data		Testing data	
			Class distribution	IR	Class distribution	IR
Worms (Ws)	'5','2','3'	900	31/46	1.48	73/108	1.48
Plane (Pl)	'3','5'	144	36/69	1.92	54/51	.944
Haptics (Ht)	'1','5'	1092	51/104	2.04	127/181	1.43
FISH	'4','5'	463	43/132	3.07	57/118	2.07
UWaveGestureLibraryAll (UWGLA)	'8','3'	945	206/690	3.35	914/2668	2.92
InsectWingbeatSound (IWS)	'1','2'	256	40/180	4.5	360/1620	4.5
Cricket_Z (CZ)	'3','5'	300	52/338	6.5	78/312	4
SwedishLeaf (SL)	'10','7'	128	54/446	8.26	96/529	5.51
FaceAll (FA)	'1','2'	131	80/480	12	210/1480	7.05
MedicalImages (MI)	'5','6','8'	99	23/358	15.57	69/691	10
ShapesAll (SA)	'1','2','3'	512	30/570	19	30/570	19
NonInvasiveFatalECG_Thorax1 (NIFT)	'1','23'	750	71/1729	24.35	100/1865	18.65

IR is the imbalance ratio (#majority class samples/#minority class samples).

**Base classifier.** Previous studies [10-11,18] have been shown that Support Vector Machines (SVM) in conjunction with the oversampling technique SPO (/INOS/MoGT) can acquire better performance in terms of F1 and G-mean than the state-of-the-art approaches 1NN and 1NN-DTW [45] for classifying imbalanced time series data. Hence, we select SVM with linear kernel as base classifier for achieving the experimental comparisons.

The parameter C of SVM is optimized by a nested 5-fold cross-validation over the training data. The considered values are  $\{2^{-3}, 2^{-2}, \dots, 2^{-10}\}$ . For each experimental dataset, the oversampling algorithm is applied to handle the training data so as to balance class distribution. Given that oversampling techniques involve into the use of random numbers. We run the oversampling method 10 times on the training data, the final performance result is the average of 10 results classifying the test data.

**Table 3:** Performance results of all the compared methods on the imbalanced unimodal datasets

Metrics	Methods	Datasets											
		Yg	Hr	Sb	POC	Lt2	PPOC	E200	Eq	TP	Car	PPOA	Wf
F1	NONE	.565	NaN	<b>.957</b>	.358	.578	.701	.714	NaN	.578	.688	.424	.316
	ROS	.607	.405	.951	<b>.564</b>	.612	.738	.743	.111	.637	.813	<b>.532</b>	.651
	SMOTE	.595	<b>.503</b>	.937	.481	<b>.696</b>	.724	.768	.195	.638	<b>.840</b>	.437	.600
	MDO	.607	.406	.948	.554	.630	.747	.734	.062	.628	.688	.496	.600
	INOS	<b>.614</b>	.417	.949	.506	.604	.743	.754	.075	.647	.781	.505	.615
	MoGT	.572	.392	.945	.535	.653	.743	<b>.774</b>	.187	.592	.688	.436	<b>.684</b>
	OHIT	.613	.466	.951	.550	.654	<b>.750</b>	.765	<b>.197</b>	<b>.649</b>	.827	.510	.561
G-mean	NONE	.618	.000	.969	.475	.639	.751	.773	.000	.682	.742	.626	.437
	ROS	.639	.509	.968	<b>.635</b>	.662	.813	.800	.266	.772	.858	.769	<b>.830</b>
	SMOTE	.623	<b>.582</b>	.960	.568	<b>.722</b>	.806	.822	.382	<b>.786</b>	<b>.882</b>	<b>.831</b>	.810
	MDO	.640	.511	.965	.630	.673	.814	.790	.184	.759	.742	.726	.813
	INOS	<b>.645</b>	.521	.967	.596	.656	.818	.809	.203	.779	.826	.776	.811

	MoGT	.607	.499	.964	.616	.689	.818	<b>.826</b>	.379	.742	.742	.718	.813
	OHIT	.642	.558	<b>.969</b>	.626	.695	<b>.822</b>	.818	<b>.396</b>	.783	.869	.793	.808
AUC	NONE	.677	.249	.990	.669	.706	<b>.904</b>	.903	.468	.850	.929	.891	.802
	ROS	.677	.617	.991	.669	.699	.884	.894	.532	.853	<b>.936</b>	.873	<b>.885</b>
	SMOTE	.662	<b>.634</b>	<b>.993</b>	.631	.722	.886	.900	<b>.566</b>	.856	.931	.901	.760
	MDO	.677	.603	.992	<b>.675</b>	<b>.727</b>	.899	.896	.531	.856	.926	.900	.875
	INOS	<b>.686</b>	.621	.992	.651	.700	.888	.892	.532	<b>.863</b>	.931	.908	.863
	MoGT	.637	.624	.989	.670	.701	.888	<b>.913</b>	.527	.820	.907	.896	.758
	OHIT	.682	.627	.992	.665	.706	.899	.901	.534	.860	.934	<b>.910</b>	.871

Best (/Worst) results are highlighted in bold (/italics) Type.

### 3.2 Comparison of Oversampling Methods

To evaluate the effectiveness of OHIT, we compare OHIT with existing representative oversampling methods, including random oversampling ROS, interpolation-based synthetic oversampling SMOTE, structure-preserving oversampling MDO and INOS, and the mixture model of Gaussian trees MoGT. With respect to the setting of parameters, the parameter values of OHIT are  $k1 = 1.5\sqrt{n}$ ,  $\kappa = \sqrt{n}$ , and  $drT = 0.9$ , where  $n$  is the number of minority samples. All the other methods use the default values recommended by the corresponding authors. Specifically, the neighbor parameter  $K$  of SMOTE is set to 5; the parameters  $K1$  and  $K2$  in MDO are 5 and 10, respectively; for INOS, 70% of the synthetic samples are generated from the Gaussian distribution reflecting the covariance structure of minority class (i.e.,  $r = 0.7$ ); in MoGT, the Bayesian information criterion is used to determine the number of mixture components.

Tables 3 and 4 respectively present the classification performances of all the compared algorithms on the unimodal datasets and multimodal datasets, where *original* represents SVM without combining any oversampling. In order to verify whether OHIT can significantly outperform the other compared algorithms, we perform the Wilcoxon signed-ranks test on the classification results of Tables 3 and 4. The test results are summarized in Table 5, where “+” and “\*” denote the corresponding p value is not greater than 0.05 and 0.1, respectively. From Table 5, one can see that the  $p$  values on most of the significant tests are not beyond 0.05, and there are more significant differences on the multimodal datasets in comparison with the unimodal datasets.

**Table 4:** Performance results of all the compared methods on the imbalanced multimodal datasets

Metrics	Methods	Datasets											
		Ws	Pl	Ht	FISH	UWG LA	IWS	CZ	SL	FA	MI	SA	NIFT
F1	NONE	.027	.962	.439	.863	.718	.618	NaN	.367	.826	.200	.667	<b>.735</b>
	ROS	.464	.967	.537	<b>.900</b>	.653	.585	.370	<b>.812</b>	<b>.834</b>	.351	.478	.695
	SMOTE	.505	<b>.980</b>	.622	.875	.705	.660	<b>.553</b>	.639	.810	.393	.475	.354
	MDO	.493	.972	.608	.884	.676	.675	.431	.733	.819	<b>.610</b>	.684	.646
	INOS	.468	.968	.592	.896	.735	.685	.473	.786	.815	.436	.476	.680
	MoGT	.468	.975	.615	.888	.728	<b>.696</b>	.390	.787	.756	.443	.620	.587
	OHIT	<b>.505</b>	.967	<b>.629</b>	.893	<b>.741</b>	.683	.515	.787	.811	.449	<b>.687</b>	.693
G-mean	NONE	.117	.962	.539	.875	.793	.708	.000	.478	.877	.358	.729	.804
	ROS	.549	.967	.612	<b>.922</b>	.767	.772	.530	.878	.886	.633	.867	.807
	SMOTE	.568	<b>.980</b>	.672	.918	.836	.844	<b>.754</b>	.875	<b>.904</b>	.756	.911	<b>.879</b>
	MDO	.572	.972	.667	.900	.786	.798	.599	.848	.888	.773	.930	.786
	INOS	.553	.968	.654	.916	.842	.847	.642	.890	.901	.766	.900	.837

	MoGT	.553	.975	.673	.905	.829	.841	.576	.905	.887	.739	.908	.803
	OHIT	<b>.577</b>	.967	<b>.684</b>	.913	<b>.845</b>	<b>.850</b>	.691	<b>.907</b>	.900	<b>.780</b>	<b>.931</b>	.852
AUC	NONE	.436	.998	.710	.950	.907	.884	.735	.959	.960	.856	.927	.961
	ROS	.555	.996	.674	.949	.863	.839	.721	.951	<b>.961</b>	.712	.911	.971
	SMOTE	<b>.574</b>	.998	.713	.950	.909	.898	<b>.822</b>	.944	.953	.798	.924	.953
	MDO	.559	.999	.711	.946	.877	.875	.760	.921	.954	.805	.933	.968
	INOS	.565	.996	.708	<b>.952</b>	.907	.901	.774	.949	.953	.855	.921	.972
	MoGT	.560	.997	.711	.945	.910	.896	.695	.939	.939	.838	.927	.956
	OHIT	.571	<b>.999</b>	<b>.729</b>	.951	<b>.911</b>	<b>.901</b>	.814	<b>.961</b>	.954	<b>.877</b>	<b>.936</b>	<b>.973</b>

Best (/Worst) results are highlighted in bold (/italics) Type.

It is worth noting that the significant difference has not been found between OHIT and SMOTE over the unimodal data group. To more granularly investigate the performance differences of these two algorithms, we compute the recall, specificity, and precision values of them on the unimodal datasets. The results are summarized in Table 6. According to Table 6, SMOTE performs better in recall, but does not statistically outperform OHIT in terms of recall; while OHIT obtains the higher specificity and precision values on most of the datasets, and is significantly better than SMOTE in specificity (/precision) at a significant level of 0.05 (/0.1). From this result, we can find that, compared to OHIT, SMOTE boosts the performance of minority class more aggressively, but at the same time causes the misclassification of more majority samples. One main reason may be that high dimensionality can aggravate the over-generalization problem of SMOTE. Since the space between two minority samples is increased exponentially with dimensionality, the synthetic samples interpolated by SMOTE can fall in huge region in high-dimensional space. Greatly expanding the minority class regions is beneficial to predict the minority samples, but it can also increase the risk of invading majority class regions.

**Table 5:** Summary of  $p$ -values of Wilcoxon significance tests between OHIT and each of the other compared methods

OHIT vs	Unimodal data			Multimodal data		
	F1	G-mean	AUC	F1	G-mean	AUC
Original	<b>9.8e - 4<sub>+</sub></b>	<b>9.8e - 4<sub>+</sub></b>	<b>0.0552<sub>*</sub></b>	<b>0.0122<sub>+</sub></b>	<b>4.9e - 4<sub>+</sub></b>	<b>0.0044<sub>+</sub></b>
ROS	0.4131	<b>0.0342<sub>+</sub></b>	<b>0.0425<sub>+</sub></b>	<b>0.042<sub>+</sub></b>	<b>0.0015<sub>+</sub></b>	<b>0.0034<sub>+</sub></b>
SMOTE	0.6772	.9097	.3013	<b>0.0342<sub>+</sub></b>	0.6221	<b>0.0342<sub>+</sub></b>
MDO	<b>0.0342<sub>+</sub></b>	<b>0.0093<sub>+</sub></b>	.377	.1099	<b>0.0015<sub>+</sub></b>	<b>0.0024<sub>+</sub></b>
INOS	<b>0.0342<sub>+</sub></b>	<b>0.0049<sub>+</sub></b>	<b>0.021<sub>+</sub></b>	<b>0.0425<sub>+</sub></b>	<b>0.0068<sub>+</sub></b>	<b>0.0015<sub>+</sub></b>
MoGT	<b>0.064<sub>*</sub></b>	<b>0.0122<sub>+</sub></b>	<b>0.0269<sub>+</sub></b>	<b>0.0269<sub>+</sub></b>	<b>0.0015<sub>+</sub></b>	<b>4.9e - 4<sub>+</sub></b>

**Table 6:** Recall, specificity, and precision of SMOTE and OHIT on the imbalanced unimodal datasets

Metrics	Methods	Datasets											
		Yg	Hr	Sb	POC	Lt2	PPOC	E200	Eq	TP	Car	PPOA	Wf
Recall	SMOTE	.590	<b>.477</b>	<b>.991</b>	.486	.679	<b>.808</b>	<b>.864</b>	.167	<b>.868</b>	<b>.842</b>	<b>.847</b>	.713
	OHIT	<b>.605</b>	.404	.985	<b>.559</b>	<b>.589</b>	.796	.806	<b>.185</b>	.771	.816	.694	<b>.732</b>
Specificity	SMOTE	.658	.713	.930	.664	.770	.805	.783	<b>.879</b>	.712	.924	.816	<b>.919</b>
	OHIT	<b>.682</b>	<b>.774</b>	<b>.952</b>	<b>.703</b>	<b>.821</b>	<b>.849</b>	<b>.831</b>	.849	<b>.796</b>	<b>.927</b>	<b>.907</b>	.893
Precision	SMOTE	.600	.533	.888	.477	.716	.658	.692	<b>.235</b>	.505	<b>.838</b>	.295	<b>.518</b>
	OHIT	<b>.622</b>	<b>.551</b>	<b>.920</b>	<b>.542</b>	<b>.737</b>	<b>.709</b>	<b>.729</b>	.212	<b>.561</b>	.838	<b>.403</b>	.455

In terms of recall, specificity and precision, *p*-values of Wilcoxon test between OHIT and SMOTE are 0.1763, 0.0161, and 0.0674, respectively.

Although the major advantage of OHIT is capable of dealing with the multimodality of minority class, OHIT also exhibits the performance superiority on the unimodal datasets in comparison with MDO and INOS (Table 5). A congenital deficiency of MDO is that the covariance structure of minority class adopts the sample covariance matrix. INOS uses a regularization procedure to fix the unreliable eigenspectrum of sample covariance matrix, but does not consider the negative influence of outliers for the estimation of covariance matrix. Compared to INOS, OHIT can utilize DRSNN clustering to eliminate the outliers of minority class.

**Table 7:** Average performance of OHIT and its variants across all the datasets within each group

OHIT vs	Unimodal data			Multimodal data		
	F1	G-mean	AUC	F1	G-mean	AUC
OHIT/DRSNN	.6229	.7290	.7935	.6641	.8131	.8751
OHIT/shrinkage	.5988	.6977	.7938	.6523	.7769	.8475
OHIT with ER	.5938	.6974	.7939	.6619	.7900	.8519
OHIT	<b>.6243</b>	<b>.7316</b>	<b>.7984</b>	<b>.6966</b>	<b>.8247</b>	<b>.8813</b>

#### 4 Conclusion

The learning from imbalanced time-series data is challenging, since time series data tends to be high-dimensional and highly correlated in variables. In this study, we have proposed a structure preserving oversampling OHIT for the classification of imbalanced time-series data. To acquire the covariance structure of minority class correctly, OHIT leverages a DRSNN clustering algorithm to capture the multimodality of minority class in high-dimensional space, and uses the shrinkage technique of covariance matrix to alleviate the problem of limited samples.

Extensive experiments have been conducted to evaluate the effectiveness of OHIT on both the unimodal datasets and multimodal datasets. In most of case, OHIT can significantly outperform existing representative oversampling solutions in terms of F1, G-mean, and AUC (Table 5).

**Acknowledgement:** We thank the authors of MDO, INOS, and MoGT for sharing their algorithm codes with us.

**Funding Statement:** This work was supported in part by the National Natural Science Foundation of China (Grant NO: 62006030, 61906167), in part by the National Natural Science Foundation of Hunan Province, China (Grant NO: 2020JJ5623, 2020JJ4648), in part by the Scientific Research Foundation of Hunan Provincial Education Department (Grant NO: 20B059, 20B060, 19A048).

**Conflicts of Interest:** The authors declare that they have no conflicts of interest to report regarding the present study.

#### References

- [1] C. L. Castro and A. P. Braga, "Novel cost-sensitive approach to improve the multilayer perceptron performance on imbalanced data," *IEEE transactions on neural networks and learning systems*, vol. 24, no. 6, pp. 888-899, 2013.
- [2] N. V. Chawla, K. W. Bowyer, L. O. Hall and W. P. Kegelmeyer, "SMOTE: synthetic minority over-sampling technique," *Journal of Artificial Intelligence Research*, vol. 16, no. 1, pp. 321-357, 2002.
- [3] Z. Liu, W. Gao, Z. Gao, J. Bian, and H. Chen et al, "Self-paced ensemble for highly imbalanced massive data classification," in *Proc. ICDE*, Dallas, TX, USA, pp. 841-852, 2020.
- [4] K. E. Bennin, J. Keung, P. Phannachitta, A. Monden and S. Mensah, "Mahakil: Diversity based oversampling

- approach to alleviate the class imbalance issue in software defect prediction,” *IEEE Transactions on Software Engineering*, vol. 44, no. 6, pp. 534-550, 2017.
- [5] Y. Wang, W. Gan, J. Yang, W. Wu and J. Yan, “Dynamic curriculum learning for imbalanced data classification” in *Proc. ICCV*, Seoul, Korea, pp. 5017-5026, 2019.
  - [6] Z. H. Zhou and X. Y. Liu, “Training cost-sensitive neural networks with methods addressing the class imbalance problem,” *IEEE Transactions on knowledge and data engineering*, vol. 18, no. 1, pp. 63-77, 2005.
  - [7] T. F. Zhu, Y. P. Lin and Y. H. Liu, ”Synthetic minority oversampling technique for multiclass imbalance problems,” *Pattern Recognition*, vol. 72, no. 2017, pp. 327-340, 2017.
  - [8] T. F. Zhu, Y. P. Lin and Y. H. Liu, ”Improving interpolation-based oversampling for imbalanced data learning,” *Knowledge-Based Systems*, 2020, vol. 187, pp. 104826.
  - [9] P. Lim, C. K. Goh and K. C. Tan, “Evolutionary cluster-Based synthetic oversampling ensemble (ECO-Ensemble) for Imbalance Learning,” *IEEE Transactions on Systems, Man, and Cybernetics*, vol. 47, no. 9, pp. 2850–2861, 2017.
  - [10] H. Cao, X. L. Li, Y. K. Wood and S. K. Ng, ” SPO: structure preserving oversampling for imbalanced time series classification,” in *Proc. ICDM*, Vancouver, BC, Canada, pp. 1008-1013, 2011.
  - [11] H. Cao, X. L. Li, D. Y. W. Woon and S. K. Ng, “Integrated oversampling for imbalanced time series classification,” *IEEE Transactions on Knowledge and Data Engineering*, vol. 25, no. 12, pp. 2809–2822, 2013.
  - [12] A. Liu, J. Ghosh and C. E. Martin, ”Generative Oversampling for Mining Imbalanced Datasets,” in *DMIN*, pp.66-72, 2007.
  - [13] Y. Xie, L. Peng, Z. Chen, B. Yang and H. Zhang, ”Generative learning for imbalanced data using the Gaussian mixed model,” *Applied Soft Computing*, vol. 79, pp. 439–451, 2017.
  - [14] B. Das, N. C. Krishnan and D. J. Cook, “RACOG and WRACOG: two probabilistic oversampling techniques.” *IEEE Transactions on Knowledge and Data Engineering*, vol. 27, no. 1, pp. 222–234, 2015.
  - [15] K. Fukunaga, “Introduction to statistical pattern recognition,” Elsevier, 2<sup>nd</sup>ed, San Diego Press, 2013.
  - [16] L. Abdi and S. Hashemi, “To combat multi-class imbalanced problems by means of over-sampling techniques,” *IEEE Transactions on Knowledge and Data Engineering*, vol. 28, no. 1, pp. 238–251, 2016.
  - [17] H. F. Jerome, “Regularized discriminant analysis,” *Journal of the American statistical association*, vol. 84, no. 405, pp. 165-175, 1989.
  - [18] H. Cao, V. Y. Tan, and J. Z. Pang, “A parsimonious mixture of Gaussian trees model for oversampling in imbalanced and multimodal time-series classification,” *IEEE Transactions on Neural Networks and Learning Systems*, vol. 25, no. 12, pp. 2226–2239, 2014.
  - [19] H. Guo, Y. J. Li, S. Jennifer, M. Y. Gu, Y. Y. Huang et al, “Learning from class-imbalanced data: review of methods and applications,” *Expert Systems with Applications*, vol. 73, pp. 220–239, 2017.
  - [20] S. Braua, M. M. Islam, X. Yao and K. Murase, “MWMOTE--majority weighted minority oversampling technique for imbalanced data set learning,” *IEEE Transactions on knowledge and data engineering*, vol. 26, no. 2, pp. 405–425, 2012.
  - [21] G. Douzas, B. Fernando and F. Last, “Improving imbalanced learning through a heuristic oversampling method based on k-means and SMOTE,” *Information Sciences*, vol. 465, pp. 1–20, 2018.
  - [22] L. Cao and Y. K. Zhai, “ An over-sampling method based on probability density estimation for imbalanced datasets classification,” In *Proceedings of the International Conference on Intelligent Information Processing*, New York, NY, United States, pp. 1-6, 2016.
  - [23] T. Guo, X. Zhu, Y. Wang and F. Chen, ”Discriminative sample generation for deep imbalanced learning,” in *Proc. IJCAI*, Macao, China, 2019.
  - [24] F. Zhou, S. Yang, H. Fujita, D. Chen and C. When, “Deep learning fault diagnosis method based on global optimization GAN for unbalanced data.” *Knowledge Based Systems*, vol. 187, pp. 104837, 2020.
  - [25] Z. Xie, L. Jiang, T. Ye and X. Li, “A synthetic minority oversampling method based on local densities in low-dimensional space for imbalanced learning,” in *International Conference on Database Systems for Advanced Applications*, Springer, Cham, 2015.
  - [26] S. Bej, N. Davtyan, M. Wolfien, and O. Wolkenhauer, “LoRAS: an oversampling approach for imbalanced datasets,” *Machine Learning*, vol. 110, no. 2, pp. 1-23, 2021.
  - [27] L. Yang, Y. Guo and J. Cheng, “Manifold distance-based over-sampling technique for class imbalance learning,” In *Proc. AAAI*, Honolulu, Hawaii, USA, pp. 10071-10072, 2019.
  - [28] Douzas, Georgios and F. Bacao, “Self-organizing map oversampling (SOMO) for imbalanced data set learning,” *Expert Systems With Applications*, vol. 82, pp. 40–52, 2017.
  - [29] J. Mathew, C. K. Pang, M. Luo and W. H. Leong, “Classification of imbalanced data by oversampling in kernel space of support vector machines,” *IEEE Transactions on Neural Networks*, vol. 29, no. 9, pp. 4065–4076,

2018.

- [30] C. Bellinger, S. Sharma, N. Japkowicz and O. R. Zaane, "Framework for extreme imbalance classification: SWIM—sampling with the majority class," *Knowledge and Information Systems*, vol. 62, no. 3, pp. 841–866, 2020.
- [31] X. Tao, Q. Li, C. Ren, W. Guo, C. Li, Q. He et al, "Real-value negative selection over-sampling for imbalanced data set learning," *Expert Systems With Applications*, vol. 129, pp. 118–134, 2019.
- [32] L. Ertoz, M. Steinbach and V. Kumar, "A new shared nearest neighbor clustering algorithm and its applications," in *2nd SIAM international conference on data mining*, pp.105–115, 2002.
- [33] L. Ertoz, M. Steinbach and V. Kumar, "Finding clusters of different sizes, shapes, and densities in noisy, high dimensional data," In *Proc. ICDM*, San Francisco, CA, USA, pp. 47:58, 2003.
- [34] Jarvis, R. Austin and E.A. Patrick, "Clustering using a similarity measure based on shared near neighbors," *IEEE Transactions on computers*, vol. 100, no. 11, pp. 1025-1034, 1973.
- [35] M .E. Houle, H. P. Kriegel, P. Kroger, E. Schubert and A. Zimek, "Can shared-neighbor distances defeat the curse of dimensionality?," in *International Conference on Scientific and Statistical Database Management*, Springer, Berlin, Heidelberg, pp. 482-500, 2010.
- [36] M. Ester, H. P. Kriegel, J. Sander and X. Xu, "A density-based algorithm for discovering clusters in large spatial databases with noise," In *Proc. KDD*, vol. 96, no. 34, pp. 226-231, 1996.
- [37] Y. Zhu, M. T. Kai and M. J. Carman, "Density-ratio based clustering for discovering clusters with varying densities," *Pattern Recognition*, vol. 60, pp. 983-997, 2016.
- [38] J. Sander, M. Ester, H.P. Kriegel and X.W. Xu, "Density-based clustering in spatial databases: The algorithm gdbscan and its applications," *Data Mining Knowledge Discovery*, vol. 2, no. 2, pp. 169-194, 1998.
- [39] O. Ledoit and M. Wolf, "Honey, I shrunk the sample covariance matrix," *Social Science Electronic Publishing*, vol.30, no. 4, pp. 110-119, 2003.
- [40] S. Julisne and K. Strimmer, "A shrinkage approach to large-scale covariance matrix estimation and implications for functional genomics," *Statistical applications in genetics and molecular biology*, vol.4, no. 1, 2005.
- [41] O. Ledoit and M. Wolf, "Improved estimation of the covariance matrix of stock returns with an application to portfolio selection," *Journal of Empirical Finance*, vol. 10, no. 5, pp. 603-621, 2003.
- [42] W. F. Sharpe, "A Simplified Model for Portfolio Analysis," *Management Science*, vol. 9, no. 2, pp. 277-293, 1963.
- [43] Y. P. Chen, E. Keogh, B. Hu, N. H. Begum, A. Bagnall et al, The ucr time series classification archive, 2015. Available: [http://www.cs.ucr.edu/~eamonn/time\\_series\\_data/](http://www.cs.ucr.edu/~eamonn/time_series_data/)
- [44] Fawcett and Tom, "ROC graphs: notes and practical considerations for researchers," *Machine learning*, vol. 31, no. 1, pp. 1-38, 2004.
- [45] X. Xi, E. Keogh, C. Shelton, L. Wei and C. A. Ratanamahatana, "Fast time series classification using numerosity reduction," in *Proceedings of the 23rd international conference on Machine learning*, New York, NY, USA, PP. 1033-1040, 2006.
- [46] M. Galar, A. Fernandez, E. Barrenechea, H. Bustince and F. Herrera, "A review on ensembles for the class imbalance problem: bagging-, boosting-, and hybrid-based approaches," *IEEE Transactions on Systems, Man, and Cybernetics, Part C*, vol. 42, no. 4, pp. 463-484, 2011.
- [47] J. Lines, S. Taylor and A. Bagnall, "Time series classification with hive-cote: the hierarchical vote collective of transformation-based ensembles," *ACM transactions on knowledge discovery from data*, vol. 12, no. 5, pp. 1-35, 2018.
- [48] A. Shifaz, C. Pelletier, F. Petitjean and G. I. Webb, "Ts-chief: a scalable and accurate forest algorithm for time series classification", *Data Mining and Knowledge Discovery*, vol. 34, no. 9, pp. 742-775, 2020.